Immune gene expression profiles in high-grade urothelial carcinoma of the bladder: a NanoString study

Ekaterina Olkhov-Mitsel ,[1] Anjelica Hodgson ,[1,2] Stanley K Liu,[3] Danny Vesprini,[3] Jane Bayani,[4] John Bartlett,[4] Bin Xu,[5] Michelle R Downes[6]

[1]Laboratory Medicine and Molecular Diagnostics, Sunnybrook Health Sciences Centre, Toronto, Ontario, Canada
[2]Laboratory Medicine and Pathobiology, University of Toronto, Toronto, Ontario, Canada
[3]Radiation Oncology, Sunnybrook Health Sciences Centre, Toronto, Ontario, Canada
[4]Diagnostic Development, Ontario Institute for Cancer Research, Toronto, Ontario, Canada
[5]Pathology, Memorial Sloan Kettering Cancer Center, New York, New York, USA
[6]Pathology, Sunnybrook Health Sciences Centre, Toronto, Ontario, Canada

Correspondence to
Dr Michelle R Downes, Laboratory Medicine and Molecular Diagnostics, Sunnybrook Health Sciences Centre, Toronto, Canada; michelle.downes@sunnybrook.ca

Received 6 April 2020
Revised 29 April 2020
Accepted 1 May 2020
Published Online First 29 May 2020

To cite: Olkhov-Mitsel E, Hodgson A, Liu SK, *et al*. *J Clin Pathol* 2021;**74**:53–57.

ABSTRACT

Aims The advent of immune checkpoint inhibitor therapy has proven beneficial in a subset of high-grade urothelial carcinomas (HGUC) of the bladder. Although treatment selection is currently largely determined by programmed death-ligand 1 (PD-L1) status, multiple factors in the immune system may modulate the host immune response to HGUC and immunotherapy. In this pilot study, we used a transcriptomic approach to identify the immune milieu associated with PD-L1 expression to enhance our understanding of the HGUC immune evasion network.

Methods The immune transcriptome of 40 HGUC cystectomy cases was profiled using the NanoString nCounter Human V.1.1 PanCancer Panel. All cases were assessed for associated PD-L1 status (SP263) using whole tissue sections. PD-L1 status was determined as high or low using 25% tumour and/or immune cell staining.

Results The most significantly differentially expressed gene was PD-L1 messenger RNA (*CD274*), which strongly correlated with protein expression (r=0.720, p<0.001). The sensitivity, specificity, positive and negative predictive values of *CD274* for PD-L1 expression were 85%, 96%, 92% and 93%, respectively. The PD-L1 associated gene signature also included complement components *C1QA* and *CD46* and *NOD2* (innate immune system), proinflammatory cytokines *CXCL14, CXCL16, CCL3, CCL3L1* and *OSM* along with the immune response mediator *SMAD3,* among others. Pathway analysis determined enrichment of these genes in interleukin-10 production, lymphocyte chemotaxis and aberrant IFNγ, NF-κB and ERK signalling networks.

Conclusions We report key genes and pathways in the immune transcriptome and their association with PD-L1 status, which may be involved in immune evasion of HGUC and warrants further investigation.

INTRODUCTION

Patients diagnosed with high-grade muscle invasive urothelial carcinoma of the bladder (HGUC) have high rates of disease recurrence, progression and mortality despite optimal treatment with surgery (European Association of Urology and American Urology Association guidelines) and/or neoadjuvant and adjuvant therapy.[1–5] Thus, novel therapeutic strategies for HGUC patients are being actively explored.

Recent advancements in immunology have led to immunotherapy taking centre stage in the treatment of urothelial carcinoma (UC). In particular, immune checkpoint inhibitors (ICIs), such as programmed cell death protein (PD-1) and programmed death-ligand 1 (PD-L1) inhibitors, have emerged as therapeutic approaches for advanced and metastatic UC.[6–10] However, only a subset of patients benefit from these inhibitors.[11] Assessment of tumour and/or immune-cell PD-L1 expression by immunohistochemistry (IHC) is typically used as a complementary diagnostic to identify patients most likely to benefit from anti-PD-1/PD-L1 inhibitors, with better overall response rates noted in PD-L1-positive/high disease.[12] Yet, the positive and negative predictive values of PD-L1 IHC as a biomarker for anti-PD-1/PD-L1 inhibitors are suboptimal. Additionally, conflicting results have been reported regarding the correlation between PD-L1 expression and patient survival.[7 9 13–15]

We now know that the response to anti-PD1/PD-L1 therapy cannot be solely predicted by PD-L1 IHC status. PD-L1 expression can be transient and heterogeneous[12] and is modulated by numerous molecular mechanisms within the tumour and its microenvironment.[16 17] PD-L1 IHC does not take into account the state of active immune cell engagement of the PD-1/PD-L1 axis and its interaction with tumour microenvironment, nor whether other concurrent suppressive immune pathways are activated. In this regard, targeted gene expression panels have the ability to assess the tumour microenvironment and immune milieu of UCs more comprehensively.[12] A wide range of cytokines in the tumour microenvironment can promote tumour immune escape and induce the expression of PD-L1.[18] Therefore, immune gene expression profiling has the potential to ascertain the inflammatory status of a tumour by quantifying chemokines, cytokines and cell surface proteins along with *CD274* levels.

As a first step to understanding discrepancies in therapeutic response to ICI, we sought to evaluate the transcriptome of PD-L1 IHC high and PD-L1 IHC low HGUC. In this pilot study, our aims were (1) to determine the degree of concordance between PD-L1 IHC and messenger RNA (mRNA) levels of *CD274* and (2) identify whether there was a specific immune gene expression signature (eg, chemotaxis, leucocyte activation, suppression of T cell activation suppression and regulation of ERK1/ERK2 cascade) associated with PD-L1 status in HGUC.

Table 1 Clinicopathological characteristics of the cohort (n=40)

Characteristic	N (%)	
Age (years)		
Mean	69.8	
Range	33 to 88	
Sex		
Male	28	(70.0)
Female	12	(30.0)
CIS		
Present	18	(45.0)
Absent	22	(55.0)
pT stage		
pT1	1	(2.5)
pT2	0	(0.0)
pT3	29	(72.5)
pT4	10	(25.0)
AJCC stage		
I	1	(2.5)
II	0	(0.0)
III	27	(67.5)
IV	12	(30.0)
Surgical margins		
Positive	13	(32.5)
Negative	27	(67.5)
Lymphovascular invasion		
Present	29	(72.5)
Absent	11	(27.5)
Lymph node metastases		
Present	12	(30.0)
Absent	25	(62.5)
N/A	3	(7.5)

AJCC, American Joint Committee on Cancer; CIS, Carcinoma In Situ; pT, Pathologic T category.

MATERIALS AND METHODS

Case selection and review

This study was approved by the Research Ethics Board at Sunnybrook Health Sciences Centre (REB 187–2016). A subset of 40 HGUC (≥pT2) bladder cystectomy cases (1999 to 2015) was identified from a larger cohort[19] of 235 cases through a retrospective search of the laboratory information system, Sunquest CoPath. Six patients were BCG treated, all others were treatment naïve. Exclusion criteria were non-urothelial histology, presence of any neuroendocrine carcinoma component and divergent differentiation encompassing >50% of the tumour. Only tumours with clinical follow-up and sufficient tumour blocks were selected for the NanoString work. The complete set of H&E-stained slides from each cystectomy was collected and reviewed by a urological pathologist (MRD), to confirm tumour histology, grade (according to the 2016 WHO/International Society of Urological Pathology guidelines), pathological stage (American Joint Committee on Cancer immunohistochemistry (AJCC)/tumour, node, metastases (TNM) eighth edition), presence of carcinoma in situ, lymphovascular invasion, nodal metastases and margin status.

Immunohistochemistry

Whole tissue section PD-L1 expression was determined with the Ventana SP263 (Ventana Medical Systems, Tucson, Arizona, USA) antibody according to manufacturer's protocol. PD-L1 staining was scored as high when >25% tumour cells (TC) or immune cells (IC) staining was seen, according to manufacturer's recommendations. TC staining was defined as either partial or complete membranous staining of any intensity. IC staining was defined as either cytoplasmic or membranous staining of any intensity. The identification of TCs and ICs was based on morphological features on H&E-stained slides. Both TC and IC staining were assessed as either present or absent. Interpretation of immunohistochemically stained slides were conducted by one genitourinary pathologist (MRD) blinded to all case characteristics.

RNA isolation and gene expression profiling

A single representative formalin-fixed, paraffin-embedded (FFPE) tissue block stored at room temperature was selected from each case for RNA extraction and sectioned at a thickness of 5 µm (4 to 10 sections per case). Representative tumour areas were outlined on the unstained slides and macrodissected within 7 days. Total RNA was extracted from the macrodissected tissue using high-pure FFPET RNA Isolation Kit (Roche Diagnostics, Indianapolis, Indiana, USA), per manufacturer's instructions. RNA profiling was performed with 250 ng (quantified using NanoDrop-1000, Thermo Fisher Scientific, Waltham, Massachusetts, USA) of RNA using the NanoString nCounter Human V.1.1 PanCancer Immune Profiling Panel (NanoString Technologies Inc, Seattle, Washington, USA), according to the manufacturer's instructions.

Raw gene expression data was analysed using NanoString's software nSolver V.4.0 with the Advanced Analysis 2.0 plugin. Data normalisation was performed using internal negative control probes, synthetic positive controls and 36 selected housekeeping genes that were identified using the nSolver normalisation module, which uses the geNorm algorithm (https://genorm.cmgg.be/). Data was normalised using geometric mean, log2-transformed and then used as input for further analysis. P values were adjusted using the Benjamini-Hochberg (BH) method to control the false discovery rate (FDR). Statistically significant, differentially expressed genes (DEGs) were defined as those with expression levels corresponding to a log2 ratio >1 or <−1 and BH q<0.05. Functional and pathway enrichment analysis was performed using g:Profiler (V.e94_eg41_p11_9f195a1) with a BH-FDR multiple testing correction method applying significance threshold of 0.05.

Statistical analysis

All statistical analyses were performed with SPSS 24.0 (IBM Corporation, Armonk, New York, USA). Comparisons between PD-L1 expression (high, low) and continuous data were performed using the Mann-Whitney U test while comparisons between binary PD-L1 expression and categorical variables were performed using the Fisher's exact test. For all described methods, two-sided P values less than 0.05 were considered statistically significant. Correlation between PD-L1 and *CD274* expression was assessed using Pearson correlation. The continuous *CD274* expression variable was dichotomised using receiver operating characteristic (ROC) analysis. Briefly, ROC analysis was performed to determine the threshold value that allowed optimal separation between PD-L1 IHC high versus low cases with maximum combined sensitivity and specificity. The NanoString *CD274* mRNA expression threshold value used was 3.7, assigning cases into positive (RNA abundance >3.7) and negative (RNA abundance <3.7) groups. Sensitivity, specificity, positive and negative predictive values were calculated using this cut-off with true positive defined as PD-L1 IHC high, true negative defined as PD-L1 IHC low, false positive defined as *CD274* mRNA expression positive but PD-L1 IHC low and false negative defined as *CD274* mRNA expression negative but PD-L1 IHC high.

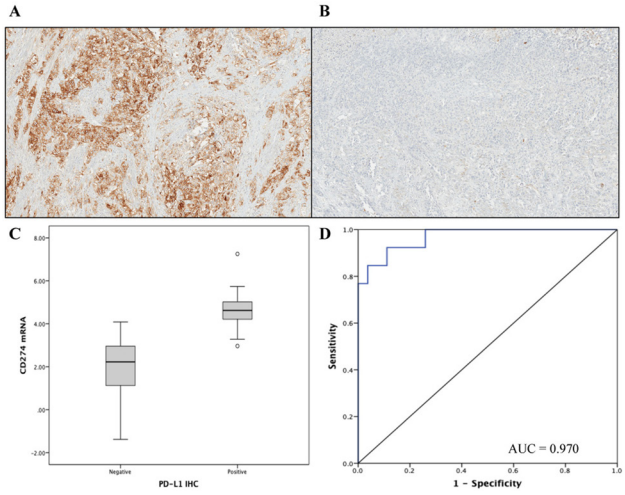

Figure 1 (A) High and (B) low PD-L1 immunoexpression (Ventana SP263 IHC assay), compared with (C) mRNA expression of *CD274* in PD-L1 high versus PD-L1 low high-grade urothelial carcinomas of the bladder, box and whisker plot. (D) Receiver operating characteristic (ROC) curve illustrating the performance of *CD274* mRNA expression in predicting PD-L1 protein detection by IHC. The sensitivity, specificity, positive and negative predictive values of PD-L1 mRNA expression for protein detection by IHC, using the optimal cut-off 3.7 (maximum combined sensitivity and specificity), were 85%, 96%, 92% and 93%, respectively. AUC, area under the curve; IHC,immunohistochemistry; mRNA, messenger RNA; PD-L1, programmed death-ligand 1.

RESULTS

The study population was composed of 40 patients with HGUC of bladder (≥pT2) treated by cystectomy (1999 to 2015). Clinicopathological parameters of the cohort are summarised in table 1. No patients received neither neoadjuvant nor adjuvant immunotherapy.

Correlation of *CD274* mRNA and PD-L1 protein expression

We examined the relationship between PD-L1 protein expression detected by IHC and *CD274* mRNA (which encodes the PD-L1 protein) expression levels (figure 1C). We found *CD274* mRNA strongly correlated with PD-L1 protein expression (Pearson's correlation coefficient r=0.720, p<0.001). ROC analysis was then performed to determine the optimal threshold of *CD274* mRNA expression level to predict the PD-L1 IHC results (high vs low) with maximum combined sensitivity and specificity. The NanoString *CD274* RNA abundance level threshold value was determined to be 3.7. Sensitivity, specificity, positive and negative predictive values of *CD274* expression for PD-L1 protein detection by IHC at this cut-off were 85%, 96%, 92% and 93%, respectively (figure 1D). IHC and RNA profiling were discordant in three (8%) HGUC cases. Of these, two were PD-L1 IHC high based solely on IC staining while the *CD274* mRNA expression in these cases was below the RNA expression cut-off value determined by ROC.

Identification of an immune gene expression signature associated with PD-L1 expression

To characterise the immune milieu associated with PD-L1 IHC in our cohort, gene expression profiles were analysed using an immune cancer gene panel of 770 genes (NanoString Technologies). More concretely, we sought to identify genes with differential expression values between PD-L1 IHC high and PD-L1 IHC low samples which would allow us to delineate which genes in the immune transcriptome are informative of PD-L1 mediated immune evasion. We found that PD-L1 protein expression is associated with a gene signature containing 16 significantly DEGs (table 2, figure 2A). As expected, the most significantly differentially expressed gene was *CD274* (encodes PD-L1).

Pathway analysis (figure 2B) determined enrichment of these 16 DEGs in production of interleukin-10 (eg, *CD46*, *NOD2*) previously shown to induce PD-L1 expression, lymphocyte chemotaxis (eg, *CXCL14*, *CXCL16*), leucocyte activation (eg, *CD46*, *NOD2*), suppression of T cell activation (eg, *FCER1G*, *PDCD1LG2*) and regulation of ERK1/ERK2 cascade (eg, *CXCL16*, *CCL3*) known to be involved in PD-L1 upregulation. Notably, *NOD2* and *FCER1G* are also involved in activation of NF-κB, a transcription factor involved in activation of PD-L1 transcription.

DISCUSSION

In this pilot study, we have shown that detection of PD-L1 RNA in FFPE clinical samples using NanoString-based profiling demonstrates high sensitivity and specificity with protein detection using a commercially available PD-L1 IHC assay (Ventana SP263). Evaluation of the immune milieu of these tumours by NanoString suggests that the key genes in the immune transcriptome that are associated with PD-L1 mediated immune evasion are complement components *C1QA* and *CD46* as well as *NOD2* signalling (innate immune system), proinflammatory cytokines *CXCL14*, *CXCL16*, *CCL3*, *CCL3L1* and *OSM* along with the immune response mediator *SMAD3* (transforming growth factor beta (TGFβ) signalling).

Our findings are in line with several other studies reporting strong correlation between PD-L1 protein IHC and mRNA measured by NanoString, RNA-seq and reverse transcription (RT)-quantitative PCR technologies.[20–23] However, others have found weak or no correlation between PD-L1 mRNA and IHC.[24 25] This is likely related to different mRNA quantification methods and IHC protocols (RNA in situ hybridisation, RT-PCR, different IHC protocols, antibody clones and quantification). In this regard, important advantages of the NanoString technology are its applicability to FFPE samples and digital counting proving a direct measurement of mRNA levels without amplification bias. Our NanoString immune transcriptome

Table 2 Differentially expressed genes between PD-L1 (SP263) high versus PD-L1 (SP263) low high-grade urothelial bladder carcinoma cases

mRNA	Linear fold change	FDR (BH) P-Value
CD274	5.6	<0.001
C1QA	3.7	0.044
PDCD1LG2	3.0	0.001
CTSH	3.0	0.047
SIGLEC1	3.0	0.007
CD46	2.9	0.002
CXCL14	2.7	0.030
CCL3	2.7	0.015
CXCL16	2.6	0.044
NOD2	2.6	0.044
OSM	2.6	0.037
LILRB1	2.5	0.044
CCL3L1	2.0	0.044
FCER1G	–2.4	0.001
C1QB	–3.3	0.009
SMAD3	–4.4	0.028

BH, Benjamini-Hochberg method; FDR, false discovery rate; mRNA, messenger RNA; PD-L1, programmed death-ligand 1.

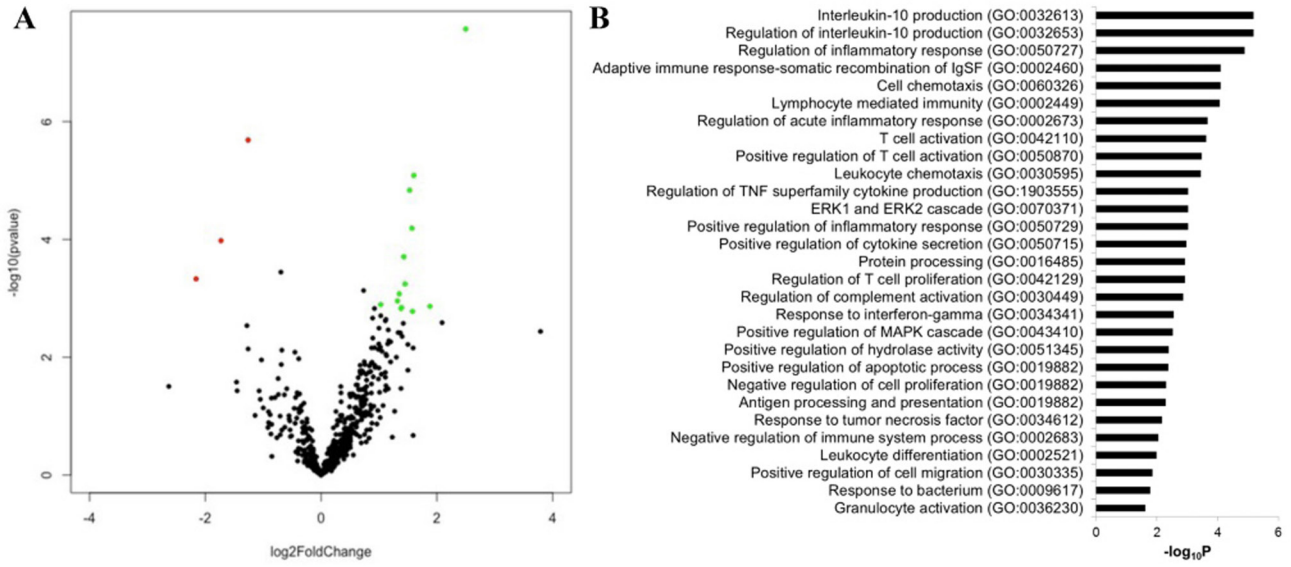

Figure 2 (A) Volcano plot of differentially expressed genes between PD-L1 (SP263) high versus low high-grade urothelial bladder carcinoma (HGUC) cases. Three genes were significantly (log2 ratio >1 and BH q value<0.05) more abundant in PD-L1 low HGUC (red data points), and 13 genes were significantly more abundant in PD-L1 high HGUC (green data points). (B) Bar graph depicting enriched GO terms by g:Profiler analysis of the 16 significantly differentially expressed genes between PD-L1 (SP263) high versus low cases. BH,Benjamini-Hochberg method; PD-L1, programmed death-ligand 1.

analysis of HGUC identified a 16 immune gene expression signature associated with PD-L1 expression. The findings indicate a cross-talk between PD-L1 in the adaptive immunosuppressive pathway and the innate immune response genes *C1QA, CD46* (complement system) and *NOD2* (NOD2 signalling). *C1QA* encodes for subunit A of the complement C1q protein, which has been shown to act as a tumour-promoting factor by promoting tumour proliferation, adhesion, migration, angiogenesis and metastasis.[26] Although the mechanism that links PD-L1 and *C1QA* gene expression has not been yet examined, it has been shown that other complement components (C3a and C5a) can induce PD-L1 expression through the activation of ERK1/ERK2 and JNK signalling pathways.[27] *CD46* is a complement regulatory protein that regulates various T-cell subsets during an active immune response.[28] Specifically, the binding of *CD46* on CD4 + Tcells has been found to promote T-helper type 1cell proliferation and activation along with upregulation of interleukin-10 (IL-10) and IFNγ, a cytokine that regulates the expression of PD-L1.[28] Another member of the innate inflammatory system, *NOD2*, is primarily involved in immune response to bacteria and viruses through the activation of IL-10, NF-κB, MAPkinase (MAPK) and caspase-1 pathways, which leads to increased expression of proinflammatory factors and PD-L1.[29 30] Notably, both *CD46* and *NOD2* have been shown to modulate expression of the cytokine IL-10. Although IL-10 itself has not been shown to directly induce the expression of PD-L1, inhibition of IL-10 in the tumour microenvironment has been linked to decreased expression of PD-L1.[18]

Studies have shown that a myriad of cytokines in the tumour microenvironment can induce the expression of PD-L1 and promote tumour immune escape.[18] In our HGUC cohort, the proinflammatory chemokines *CXCL14*, *CXCL16*, *CCL3* and *CCL3L1* as well as the OSM cytokine were all upregulated in association with PD-L1 expression, indicating a potential cross-talk between these genes in tumour immune tolerance and progression of HGUC.

The proinflammatory chemokine *CXCL14* is mainly involved in stimulating chemotaxis of various immune cells including NK cells, B cells and macrophages.[31] However, the exact molecular mechanisms by which *CXCL14* mediates immune response are unknown. To date, *CXCL14* expression has been linked to calcium influx, NF-κB activity, activation of AP-1, NOS1 and MEK-ERK. Of note, NF-κB and ERK activity has also been linked to PD-L1 expression. The chemokine *CXCL16* also induces chemotaxis and its expression has been shown to be induced by IFNγ, leading to activation of the ERK1/ERK2 signalling pathway and promotion of tumour proliferation.[32] The chemotactic proinflammatory chemokine, *CCL3*, is known to enhance leucocyte infiltration to sites of acute inflammation, as seen in cancer.[33] This is consistent with our results indicating positive correlation between *CCL3* and PD-L1 expression as tumor infiltrating lymphocytes have been shown to overexpress PD-L1 to inhibit antitumour immune response.[33] Further, we report a positive correlation between the expression of PD-L1 and the chemotactic, proinflammatory chemokine, *CCL3L1*. This chemokine has been shown to be functionally involved in proliferation of leukocytes, lymphocytes and macrophages as well as tumourigenesis of glioblastoma.[34] Lastly, we found association between expression of PD-L1 and the proinflammatory cytokine *OSM* which has been shown to stimulate several signalling pathways (Janus kinases/signal transducer and activator of transcription proteins, MAPK and PI3 kinase), some of which are involved in the upregulation of PD-L1 expression.[35] Our findings imply cross-talk between PD-L1 expression and downregulation of *SMAD3* (key component of TGFβ signalling) in inhibition of antitumour immunity. This is consistent with previous reports that *SMAD3*-deficient mice have increase in constitutively activated T cells and expression of cytokines such as IL-2, IL-13, IL-15 and IFNγ.[36]

In conclusion, we identified significant correlation between PD-L1 IHC and *CD274* mRNA levels. We further identified different gene expression profiles in PD-L1 high versus PD-L1

low HGUC. These initial findings are encouraging and warrant further exploration in ICI treated cohorts to assess how these gene expression profiles correlate with therapeutic outcome.

Take home messages

- There is a significant correlation between programmed death-ligand 1 (PD-L1) immunohistochemistry (Ventana SP263) and *CD274* messenger RNA levels (NanoString profiling) in high-grade urothelial carcinoma (HGUC) of the bladder.
- NanoString immune profiling of HGUC identified a 16 gene signature associated with PD-L1 expression including *C1QA, CD46, NOD2* (innate immune system), proinflammatory cytokines *CXCL14, CXCL16, CCL3, CCL3L1* and *OSM* along with the immune response mediator *SMAD3* (TGFβ signalling)
- Key pathways in the immune transcriptome associated with PD-L1 status are interleukin-10 production, lymphocyte chemotaxis and aberrant IFNγ, NF-κB and ERK signalling networks.

Handling editor Runjan Chetty.

Contributors MRD designed the study. AH, BX and MRD gathered the immunohistochemistry data. JB and JB performed the gene expression profiling. EO-M, AH, SKL, DV, BX and MRD reviewed and interpreted the data. EO-M performed the RNA extraction and statistical analysis. EO-M, AH, SKL, DV, BX, JB, JB and MRD contributed to drafting and review of the manuscript, and to approval of the final version.

Funding The SP263 antibody was purchased using a Sunnybrook Health Sciences Centre departmental Educational Grant courtesy of AstraZeneca.

Competing interests MRD has been an advisory board member for AstraZeneca and Hoffmann-La Roche and has received speaker's honoraria from AstraZeneca.

Patient consent for publication Not required.

Ethics approval This study was approved by the Research Ethics Board at Sunnybrook Health Sciences Centre (REB 187–2016)

Provenance and peer review Not commissioned; externally peer reviewed.

Data availability statement Data are available upon reasonable request from corresponding author.

ORCID iDs
Ekaterina Olkhov-Mitsel http://orcid.org/0000-0001-7945-7801
Anjelica Hodgson http://orcid.org/0000-0002-4069-2000

REFERENCES

1 Kirkali Z, Chan T, Manoharan M, *et al*. Bladder cancer: epidemiology, staging and grading, and diagnosis. *Urology* 2005;66:4–34.
2 Alfred Witjes J, Lebret T, Compérat EM, *et al*. Updated 2016 eau guidelines on muscle-invasive and metastatic bladder cancer. *Eur Urol* 2017;71:462–75.
3 Shariat SF, Karakiewicz PI, Palapattu GS, *et al*. Outcomes of radical cystectomy for transitional cell carcinoma of the bladder: a contemporary series from the bladder cancer research Consortium. *J Urol* 2006;176:2414–22.
4 Madersbacher S, Hochreiter W, Burkhard F, *et al*. Radical cystectomy for bladder cancer today--a homogeneous series without neoadjuvant therapy. *J Clin Oncol* 2003;21:690–6.
5 Rink M, Lee DJ, Kent M, *et al*. Predictors of cancer-specific mortality after disease recurrence following radical cystectomy. *BJU Int* 2013;111:E30–6.
6 Gopalakrishnan D, Koshkin VS, Ornstein MC, *et al*. Immune checkpoint inhibitors in urothelial cancer: recent updates and future outlook. *Ther Clin Risk Manag* 2018;14:1019–40.
7 Bellmunt J, de Wit R, Vaughn DJ, *et al*. Pembrolizumab as second-line therapy for advanced urothelial carcinoma. *N Engl J Med* 2017;376:1015–26.
8 Powles T, Eder JP, Fine GD, *et al*. MPDL3280A (anti-PD-L1) treatment leads to clinical activity in metastatic bladder cancer. *Nature* 2014;515:558–62.
9 Rosenberg JE, Hoffman-Censits J, Powles T, *et al*. Atezolizumab in patients with locally advanced and metastatic urothelial carcinoma who have progressed following treatment with platinum-based chemotherapy: a single-arm, multicentre, phase 2 trial. *Lancet* 2016;387:1909–20.
10 Suzman DL, Agrawal S, Ning Y-M, *et al*. Fda approval summary: Atezolizumab or pembrolizumab for the treatment of patients with advanced urothelial carcinoma ineligible for cisplatin-containing chemotherapy. *Oncologist* 2019;24:563–9.
11 Jenkins RW, Barbie DA, Flaherty KT. Mechanisms of resistance to immune checkpoint inhibitors. *Br J Cancer* 2018;118:9–16.
12 Aggen DH, Drake CG. Biomarkers for immunotherapy in bladder cancer: a moving target. *J Immunother Cancer* 2017;5:94.
13 Massard C, Gordon MS, Sharma S, *et al*. Safety and efficacy of durvalumab (medi4736), an anti-programmed cell death ligand-1 immune checkpoint inhibitor, in patients with advanced urothelial bladder cancer. *J Clin Oncol* 2016;34:3119–25.
14 Drake CG, Bivalacqua TJ, Hahn NM. Programmed cell death ligand-1 blockade in urothelial bladder cancer: to select or not to select. *J Clin Oncol* 2016;34:3115–6.
15 Sharma P, Retz M, Siefker-Radtke A, *et al*. Nivolumab in metastatic urothelial carcinoma after platinum therapy (CheckMate 275): a multicentre, single-arm, phase 2 trial. *Lancet Oncol* 2017;18:312–22.
16 Bai J, Gao Z, Li X, *et al*. Regulation of PD-1/PD-L1 pathway and resistance to PD-1/PD-L1 blockade. *Oncotarget* 2017;8:110693–707.
17 Zerdes I, Matikas A, Bergh J, *et al*. Genetic, transcriptional and post-translational regulation of the programmed death protein ligand 1 in cancer: biology and clinical correlations. *Oncogene* 2018;37:4639–61.
18 Jiang X, Wang J, Deng X, *et al*. Role of the tumor microenvironment in PD-L1/PD-1-mediated tumor immune escape. *Mol Cancer* 2019;18:10.
19 Hodgson A, Xu B, Downes MR. P53 immunohistochemistry in high-grade urothelial carcinoma of the bladder is prognostically significant. *Histopathology* 2017;71:296–304.
20 Brunnström H, Johansson A, Westbom-Fremer S, *et al*. Pd-L1 immunohistochemistry in clinical diagnostics of lung cancer: inter-pathologist variability is higher than assay variability. *Mod Pathol* 2017;30:1411–21.
21 Conroy JM, Pabla S, Nesline MK, *et al*. Next generation sequencing of PD-L1 for predicting response to immune checkpoint inhibitors. *J Immunother Cancer* 2019;7:18.
22 Erber R, Stöhr R, Herlein S, *et al*. Comparison of *PD-L1* mRNA Expression Measured with the CheckPoint Typer® Assay with *PD-L1* Protein Expression Assessed with Immunohistochemistry in Non-small Cell Lung Cancer. *Anticancer Res* 2017;37:6771–8.
23 Schats KA, Van Vré EA, De Schepper S, *et al*. Validated programmed cell death ligand 1 immunohistochemistry assays (E1L3N and SP142) reveal similar immune cell staining patterns in melanoma when using the same sensitive detection system. *Histopathology* 2017;70:253–63.
24 Eckstein M, Wirtz RM, Pfannstil C, *et al*. A multicenter round Robin test of PD-L1 expression assessment in urothelial bladder cancer by immunohistochemistry and RT-qPCR with emphasis on prognosis prediction after radical cystectomy. *Oncotarget* 2018;9:15001–14.
25 Kim H, Kwon HJ, Park SY, *et al*. Clinicopathological analysis and prognostic significance of programmed cell death-ligand 1 protein and mRNA expression in non-small cell lung cancer. *PLoS One* 2018;13:e0198634.
26 Bulla R, Tripodo C, Rami D, *et al*. C1Q acts in the tumour microenvironment as a cancer-promoting factor independently of complement activation. *Nat Commun* 2016;7:10346.
27 Pio R, Ajona D, Ortiz-Espinosa S, *et al*. Complementing the Cancer-Immunity cycle. *Front Immunol* 2019;10:774.
28 Geller A, Yan J. The role of membrane bound complement regulatory proteins in tumor development and cancer immunotherapy. *Front Immunol* 2019;10:1074.
29 Hewitt RE, Pele LC, Tremelling M, *et al*. Immuno-inhibitory PD-L1 can be induced by a peptidoglycan/NOD2 mediated pathway in primary monocytic cells and is deficient in Crohn's patients with homozygous NOD2 mutations. *Clin Immunol* 2012;143:162–9.
30 Negroni A, Pierdomenico M, Cucchiara S, *et al*. Nod2 and inflammation: current insights. *J Inflamm Res* 2018;11:49–60.
31 Lu J, Chatterjee M, Schmid H, *et al*. Cxcl14 as an emerging immune and inflammatory modulator. *J Inflamm* 2016;13:1.
32 Deng L, Chen N, Li Y, *et al*. CXCR6/CXCL16 functions as a regulator in metastasis and progression of cancer. *Biochim Biophys Acta* 2010;1806:42–9.
33 Huang Y, Zhang S-D, McCrudden C, *et al*. The prognostic significance of PD-L1 in bladder cancer. *Oncol Rep* 2015;33:3075–84.
34 Kouno J, Nagai H, Nagahata T, *et al*. Up-Regulation of CC chemokine, CCL3L1, and receptors, CCR3, CCR5 in human glioblastoma that promotes cell growth. *J Neurooncol* 2004;70:301–7.
35 Richards CD. The enigmatic cytokine oncostatin M and roles in disease. *ISRN Inflamm* 2013;2013:1–23.
36 Millet C, Zhang YE. Roles of Smad3 in TGF-beta signaling during carcinogenesis. *Crit Rev Eukaryot Gene Expr* 2007;17:281–93.